A Hydrophobic Cluster at the Surface of the Human Plasma Phospholipid Transfer Protein Is Critical for Activity on High Density Lipoproteins

Catherine M Desrumaux, Christine Labeur, Annick Verhee, Jan Tavernier, Joël Vandekerckhove, Maryvonne Rosseneu, Frank Peelman

THE JOURNAL OF BIOLOGICAL CHEMISTRY
Vol. 276, No. 8, Issue of February 23, pp. 5908–5915, 2001
Printed in U.S.A.

A Hydrophobic Cluster at the Surface of the Human Plasma Phospholipid Transfer Protein Is Critical for Activity on High Density Lipoproteins*

Received for publication, September 14, 2000, and in revised form, November 15, 2000
Published, JBC Papers in Press, November 16, 2000, DOI 10.1074/jbc.M008420200

Catherine Desrumaux‡§, Christine Labeur‡, Annick Verhee¶, Jan Tavernier¶, Joël Vandekerckhove¶, Maryvonne Rosseneu‡, and Frank Peelman‡

From the ‡Laboratory for Lipoprotein Chemistry and the ¶Flanders Interuniversity Institute for Biotechnology, Department of Biochemistry, Faculty of Medicine, University of Ghent, B-9000 Ghent, Belgium

The plasma phospholipid transfer protein (PLTP) belongs to the lipid transfer/lipopolysaccharide binding protein (LT/LBP) family, together with the cholesteryl ester transfer protein, the lipopolysaccharide binding protein (LBP) and the bactericidal permeability increasing protein (BPI). In the present study, we used the crystallographic data available for BPI to build a three-dimensional model for PLTP. Multiple sequence alignment suggested that, in PLTP, a cluster of hydrophobic residues substitutes for a cluster of positively charged residues found on the surface of LBP and BPI, which is critical for interaction with lipopolysaccharides. According to the PLTP model, these hydrophobic residues are situated on an exposed hydrophobic patch at the N-terminal tip of the molecule. To assess the role of this hydrophobic cluster for the functional activity of PLTP, single point alanine mutants were engineered. Phospholipid transfer from liposomes to high density lipoprotein (HDL) by the W91A, F92A, and F93A PLTP mutants was drastically reduced, whereas their transfer activity toward very low density lipoprotein and low density lipoprotein did not change. The HDL size conversion activity of the mutants was reduced to the same extent as the PLTP transfer activity toward HDL. Based on these results, we propose that a functional solvent-exposed hydrophobic cluster in the PLTP molecule specifically contributes to the PLTP transfer activity on HDL substrates.

Lipoprotein metabolism is regulated by the coordinated action of several factors, including lipolytic enzymes, lecithin: cholesterol acyltransferase, cholesteryl ester transfer protein (CETP)[1] and phospholipid transfer protein (PLTP) (1). Although PLTP was originally described as a mediator facilitating phospholipid transfer between lipoprotein particles, it is now recognized as a key factor in the intravascular metabolism and remodeling of HDL (2, 3). PLTP facilitates the transfer of different compounds, including phospholipids, lipopolysaccharides, α-tocopherol, and unesterified cholesterol, among lipoprotein classes and between lipoproteins and cells (2). Besides its transfer activity, PLTP enhances formation of large-sized HDL and pre-β HDL, through apoAI release and HDL fusion (4). Although the physiological role of PLTP has not been completely defined yet, recent *in vivo* studies conducted with PLTP transgenic and knock-out mice strongly suggest that PLTP contributes to the control and regulation of HDL levels and to the generation of pre-β HDL, the initial acceptors of cellular cholesterol (3).

PLTP belongs to the lipid transfer/lipopolysaccharide binding protein (LT/LBP) family, together with CETP, lipopolysaccharide binding protein (LBP), and bactericidal permeability increasing protein (BPI) (5). CETP transfers neutral lipids, *i.e.* cholesteryl esters and triglycerides between various lipoprotein fractions, and has limited phospholipid transfer activity (6). LBP and BPI bind and transfer bacterial endotoxins and lipopolysaccharides (LPS) and thus modulate the host response to Gram-negative bacterial infection (7, 8). At the sequence level, the four LT/LBP family members share ~20% identity (5), suggesting a similar tertiary structure (9). The three-dimensional structure of BPI was recently determined by x-ray crystallography (10); this protein appears as a boomerang-shaped molecule, which consists of two symmetrical barrels connected by a linker region. Each barrel forms a hydrophobic pocket that can incorporate one phosphatidylcholine molecule. The crystal structure of BPI provides a useful framework for the modeling of the three-dimensional structure of the other members of the LT/LBP family, as well as for the investigation of their functional similarities and differences. Several structure/function studies were recently aimed at identifying the functional domains and elucidating the mechanism of action of LBP, BPI, and CETP (11–15). These results demonstrated that the activity of the lipopolysaccharide-binding and lipid transfer proteins depends not only upon their ability to accommodate specific lipid substrates but also upon their interaction with bacteria and/or lipoproteins. The molecular interaction of LBP with surface-exposed lipopolysaccharides on bacteria is critical for its activity (11), and a cluster of positively charged amino acids (Arg-94, Lys-95, and Lys-99) was recently identified as the lipopolysaccharide-binding domain of this protein (16). Based on the crystal structure of BPI, this cationic cluster is fully exposed at the N-terminal tip of the boomerang-shaped LBP model (17).

* The costs of publication of this article were defrayed in part by the payment of page charges. This article must therefore be hereby marked "*advertisement*" in accordance with 18 U.S.C. Section 1734 solely to indicate this fact.

§ To whom correspondence should be addressed: Universiteit Gent, Vakgroep Biochemie, Hospitaalstraat 13, B-9000 Gent, Belgium. Tel.: 32-9-264-92-73; Fax: 32-9-264-94-96; E-mail: desrumauxcatherine@yahoo.com.

[1] The abbreviations used are: CETP, cholesteryl ester transfer protein; apoAI, apolipoprotein AI; BPI, bactericidal permeability increasing protein; HDL, high density lipoprotein; LBP, lipopolysaccharide binding protein; LDL, low density lipoprotein; LPS, lipopolysaccharide; LT/LBP, lipid transfer/lipopolysaccharide binding proteins; $sPLA_2$, secreted phospholipase A2; PC, phosphatidylcholine; PS, phosphatidylserine; PLTP, phospholipid transfer protein; TNP-PE, 2,4,6-trinitrophenyl-phosphatidylethanolamine; VLDL, very low density lipoprotein; WT, wild-type; kb, kilobase(s); DMEM, Dulbecco's modified Eagle's medium; M/E, monomer/excimer intensity ratio.

Because PLTP activity and HDL metabolism are closely related (3), a defective binding of PLTP to its HDL substrate would have direct physiological consequences, and the factors that regulate the association of PLTP with HDL are highly relevant to lipoprotein metabolism. Although the molecular and macromolecular specificity of PLTP has been thoroughly investigated (18–21), the structure/function relationships of this protein have not been completely resolved (22), and the molecular determinants regulating the association of PLTP with lipoproteins have not been elucidated yet.

In the present study, we performed multiple sequence alignment between members of the LT/LBP family and used the coordinates of crystallized BPI to build a three-dimensional model for PLTP. The results suggest that in PLTP, a cluster of hydrophobic residues, Tyr-45, Tyr-90, Trp-91, Phe-92, Phe-93, and Tyr-94, substitutes for the positively charged LPS-binding patch located on the surface of LBP and BPI. From the engineered PLTP model and the characterization of PLTP mutants obtained by site-directed mutagenesis, we propose that this solvent-exposed hydrophobic cluster is critical for the interaction of PLTP with its preferred substrate, HDL.

MATERIALS AND METHODS

Chemicals

Egg yolk phosphatidylcholine (PC), bovine brain phosphatidylserine, 2,4,6-trinitrophenyl-phosphatidylethanolamine (TNP-PE) (used as a quencher of pyrene fluorescence in liposomes), and human serum albumin were obtained from Sigma.

1-Hexadecanoyl-2-(1-pyrenedecanoyl)-*sn*-glycero-3-phosphocholine was purchased from Molecular Probes. Phospholipid concentrations were measured by an enzymatic method using Biomérieux reagents.

Multiple Sequence Alignment and Modeling of Human PLTP

Thirteen sequences of BPI, LBP, CETP, and PLTP from various species were aligned using the ClustalW program (23) and the Hidden Markov Model method SAM-T99 (24, 25), both available on the Web. The SAM-T99 sequence alignment was plotted using the Alscript software (26), and the conservation index per residue was calculated using the AMAS program (27) also available on the Web. The working model for the human PLTP structure was built based on this alignment, and on the Protein Data Bank coordinates of the BPI protein (10), by using the HOMOLOGY software of the Insight II package (Molecular Simulations, San Diego, CA). The quality of the model was checked using WHATCHECK (28) and PROCHECK (29). When aligned with the BPI template, the PLTP sequence contains four deletions defined as loops 1, 3, 4, and 5. They were replaced by the best fitting loops found by an automatic loop search of a nonredundant Protein Data Bank data base (Fig. 1). Loop 2 contains no insertions or deletions but falls within a sequence region with weak similarity with BPI; its coordinates were copied from the BPI template. Nonconserved side chains were replaced by their best-fitting rotamers using the program SCWRL (30). The model was soaked with water, and the solvated model was then energy-minimized in steps with decreasing constraints on the conserved backbone and side chains using CDiscover (Molecular Simulations) with the CVFF force field and the cell multipole method. The model was relaxed by steepest descent and conjugate gradient minimization until a convergence of <0.5 kcal/mol/Å^2 was achieved.

The conformation of loops 1, 2, and 4 in the N-terminal "tip" of PLTP was further studied by molecular dynamics simulation as follows: all residues within 5 Å of loops 1, 2, and 4 were allowed to move, while the rest of the PLTP model was fixed. A 16-Å layer of water was created around the mobile PLTP residues, and the model was energy-minimized to converge at <0.5 kcal/mol/Å^2. During the molecular dynamics simulation, the system was equilibrated at 900 K in 5 ps, kept at 900 K for 20 ps, followed by a 10-ps dynamics simulation at 300 K. The final structure was energy-minimized by steepest descent and conjugate gradient minimization.

Site-directed Mutagenesis, Subcloning, and Transfection of COS-1 Cells

Oligonucleotides containing the desired mutations were purchased from Eurogentec (Seraing, Belgium). Each of the Tyr-45, Tyr-90, Trp-91, Phe-92, Phe-93, and Tyr-94 residues was mutated to an alanine, and restriction sites were introduced by silent mutagenesis to verify the presence of each mutation prior to subcloning.

Mutagenesis of the PLTP cDNA was carried out by using the Stratagene QuikChange site-directed mutagenesis kit. The PLTP14 vector was a kind gift from Drs. J. J. Albers and A.-Y. Tu (Seattle, WA) and was used as the template for PCR. The PCR reactions were set up according to instructions of the manufacturer using the following thermal cycling conditions: 95 °C for 1 min, 55 °C for 1 min, and 68 °C for 16 min (2 min/kb of plasmid length). After PCR and *Dpn*I digestion of the parental dam-methylated template (2 h at 37 °C), the mutant plasmids were transformed into XL1 blue *Escherichia coli* cells and resulting colonies were screened by restriction analysis.

Transient expression of the PLTP cDNA into COS-1 cells was carried out by transfection with a mixture of 2 μg of the recombinant plasmids and 8.6 μg of LipofectAMINE (Life Technologies, Inc.) in serum-free DMEM. After 5-h incubation at 37 °C, cells were washed and grown overnight in complete DMEM. DMEM was then replaced by Optimem (Life Technologies, Inc.), and media were harvested between 24 and 96 h. After 10-min centrifugation at 1000 rpm, the media were stored at −20 °C in 1-ml aliquots.

Quantification of Expressed Mutants by Western Blot

Secretion of PLTP mutants into the media of the transfected COS-1 cells was assessed by SDS-polyacrylamide gel electrophoresis separation in 10% acrylamide and by Western blotting of the media after 3-fold concentration by acetone precipitation. Serial dilutions of a plasma protein fraction with a known PLTP concentration, quantified by a previously described enzyme-linked immunosorbent assay (31), were used as standards for quantification of PLTP in the cell media.

After electrophoresis, the proteins were transferred to polyvinylidene difluoride membranes (Immobilon P transfer membranes, Millipore), which were subsequently blocked with 50 g/liter nonfat dry milk in a phosphate-buffered saline buffer containing 1 g/liter Tween 20, for 1 h at room temperature. The membranes were incubated overnight at 4 °C with rabbit anti-PLTP antibodies (a generous gift from Dr. L. Lagrost, Dijon, France) diluted in phosphate-buffered saline containing 10 g/liter human serum albumin. After incubation with horseradish peroxidase-labeled anti-rabbit IgG antibodies (Dako), blots were revealed by chemiluminescence (ECL kit, Roche Molecular Biochemicals) and scanned on a densitometer.

Isolation of Lipoproteins

Very-low density (VLDL), low density (LDL), and high density (HDL) lipoproteins were isolated at $d < 1.019$ g/ml, $1.019 < d < 1.063$ g/ml, and $1.07 < d < 1.21$ g/ml, respectively, according to standard protocols (32). Densities were adjusted by the addition of KBr. All isolated lipoproteins were dialyzed overnight against a Tris/HCl buffer (10 mM Tris, 1 mM EDTA, 3 mM NaN_3, pH 7.4).

PLTP Activity Assays

Liposomes/HDL Transfer Assay—PLTP activity was monitored by a fluorometric assay (20) in the supernatant of cells transfected with wild-type (WT) or mutated PLTP, or of nontransfected cells (mock). In this assay, the rate of phospholipid transfer is monitored by the increase of pyrene monomer fluorescence intensity upon transfer of pyrene-labeled phosphatidylcholine from quenched donors to unquenched acceptors. The molar composition of the donor liposomes consisted of 68% egg yolk PC, 17% phosphatidylserine (PS), 2.5% pyrene-labeled PC (1-hexadecanoyl-2-(1-pyrenedecanoyl)-*sn*-glycero-3-phosphocholine), and 12.5% TNP-PE (the quencher of pyrene fluorescence). 12 nmol of donor liposomes containing quenched pyrene-PC-containing liposomes was mixed with 80 nmol of unlabeled HDL used as acceptors, in the presence of cell media containing PLTP. Pyrene-PC transfer was accompanied by an increase of the monomer fluorescence intensity (excitation wavelength, 342 nm; emission wavelength, 378 nm) due to release and dequenching of the pyrene probe from the liposomes. The initial slope of the fluorescence intensity increase as a function of time represented a measure of the PLTP activity in the medium. The activity measured with mock medium was close to the spontaneous transfer activity and taken as a blank value for all activity determinations. In this assay, the volume of cell medium was adjusted to yield a value within the linear range of the fluorescence curve. The assay was calibrated by measuring the rate of transfer of ^{14}C-radiolabeled phosphatidylcholine in a plasma sample, which was subsequently used as a standard for the fluorometric measurements.

Liposomes/VLDL and Liposomes/LDL Transfer Assays—These assays were as described above, except that acceptor HDL were replaced by VLDL or LDL, containing an equivalent amount (80 nmol) of phos-

FIG. 1. **Alignment of the pig, mouse, and human PLTP sequences with those of human CETP, LBP, and BPI.** Homologous or conserved residues among the LT/LBP family members are in *gray* and *black boxes*, respectively. Residue numbers correspond to human PLTP. The positions of the five loops in the PLTP sequence are indicated by a *dotted line*. The position of secondary structure elements are indicated; α-helices are numbered from *1* to *9*, and β-sheets are drawn in *capital letters*. The residues mutated in this study are indicated with an *asterisk under* the *alignment*.

pholipids. The volume of medium used for measurements was taken within the linear range of the activity curve.

HDL/HDL Transfer Assay—We developed an "inter-HDL" transfer system in which pyrene-labeled HDLs were used as phospholipid donors while unlabeled HDLs served as acceptors.

Pyrene-labeled HDL were prepared by ethanol injection of pyrene-phosphatidylcholine. Briefly, 300 nmol of 1-hexadecanoyl-2-(1-pyrene-decanoyl)-*sn*-glycero-3-phosphocholine were dissolved in ethanol and injected into HDL (3 μmol of phospholipids) under continuous stirring. The mixture was then incubated for 6 h at 37 °C while mixing, and the HDL were reisolated by ultracentrifugation between densities 1.07 and 1.21 g/ml. 60–70% of the label was incorporated into HDL, corresponding to 6.5 mol % of HDL phospholipids.

For PLTP activity measurements, pyrene-labeled HDL (40 nmol of phospholipids) were mixed with unlabeled HDL (160 nmol of phospholipids) in the presence of either control or PLTP-containing cell culture media. Fluorescence intensities of the monomer and of the excimer were recorded at 378 and 475 nm, respectively, after 60-min incubation at 37 °C. The monomer/excimer (M/E) intensity ratio increased linearly as a function of both incubation time and PLTP amount. The increase in the M/E fluorescence intensity ratio thus represented a reliable measure of "inter-HDL" PLTP transfer activity. M/E intensity ratios measured with mock medium were used as blank values and subtracted for specific activity calculations.

HDL Size Conversion Activity of PLTP

Salt-sucrose Density Gradient Ultracentrifugation of HDL-PLTP Mixtures—Conversion of HDL particles was analyzed by incubating either control or PLTP-containing cell culture media with HDL particles (5 μg of protein) for 30 h at 37 °C. The final incubation volume was 0.6 ml, and the ratio of PLTP activity/HDL concentration was similar to that in plasma. After incubation, HDL subclasses were separated by density gradient ultracentrifugation in a salt-sucrose gradient. The gradient was prepared in 12-ml polyallomer tubes (Beckman) and consisted of 0.5 g of sucrose, 5 ml of 4 M NaCl, and 500 μl of sample, on which 6.2 ml of 0.67 M NaCl was layered. Samples were centrifuged for 66 h in a SW 41 Ti rotor (Beckman) at 10 °C and 38,000 rpm. Fractions (500 μl) were collected using an auto-densiflow system (Searle, Fort Lee, NJ). Apolipoprotein AI (apoAI) was quantified in the fractions by enzyme-linked immunosorbent assay (33). The percentage of apoAI released in the bottom fraction ($d > 1.20$ g/ml) of ultracentrifuged mixtures was used as a measure of the HDL size conversion activity of PLTP.

Determination of HDL Size by Native Polyacrylamide Gradient Gel Electrophoresis—The size distribution of HDL was determined by electrophoretic analysis on 4–20% polyacrylamide gradient gels, according to the general procedure previously described (34). The gel was run at 70 V during 1 h and then at 150 V for 20 h, in a 90 mM Tris-HCl, 80 mM boric acid, pH 8.3, buffer containing 3 mM Na-EDTA and 3 mM NaN_3. At the end of the electrophoresis, gels were stained with Coomassie Brilliant Blue G. The size distribution profiles of HDL were obtained by analysis of stained gels on a Bio-Rad GS-670 imaging densitometer. The apparent diameters of HDL were determined by comparison with a calibration curve constructed with albumin (7.1 nm), lactate dehydrogenase (8.2 nm), ferritin (12.2 nm), and thyroglobulin (17.0 nm).

Statistical Analysis

Data are expressed as mean ± S.D. or mean ± S.E., as indicated in the legend of the figures. The statistical significance of differences between data means was determined using the Student's *t* test.

RESULTS

Multiple Sequence Alignment and Building of the PLTP Model—In the aligned sequences of human CETP, LBP, BPI, and of pig, mouse, and human PLTP, shown in Fig. 1, only 22 residues are strictly conserved among all sequences. The sequence alignment of human PLTP and BPI shown in Fig. 1 is practically identical to that used by Huuskonen *et al.* (22) for the modeling of PLTP. As described by these authors (22), most secondary structure elements are well conserved within this protein family. Compared with the human BPI sequence, PLTP contains four deletions, which occur in the surface loops con-

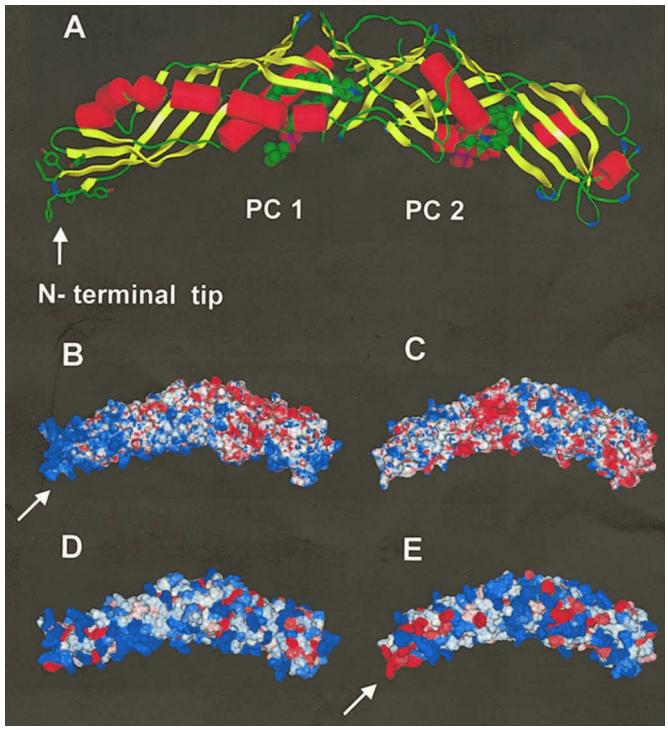

FIG. 2. **Structural model of human PLTP and molecular surface representations of human BPI (*B* and *D*) and PLTP (*C* and *E*).** *A*, PLTP model, showing the mutated aromatic residues in the N-terminal tip. In *B* and *C*: electrostatic surface potentials, calculated with Delphi (52). The positive and negative electrostatic surface potentials of BPI (*B*) and PLTP (*C*) are *blue* and *red*, respectively. In *D* and *E*: The residues were *colored* according to the Wimley and White (41) hydrophobicity scale. The hydrophilic and hydrophobic surface areas of BPI (*D*) and PLTP (*E*) are *blue* and *red*, respectively. *White arrows* in *B* and *E* point to the positively charged cluster of BPI and to the hydrophobic cluster of PLTP, respectively.

necting β-strands and α-helices. Based on the BPI coordinates, a model was built for human PLTP (Fig. 2*A*). The central part of the boomerang-shaped model structure of PLTP, containing the linker domain and the hypothetical lipid-binding pockets (22), is better conserved than the boomerang tips, which contain three of the four deletions. The N-terminal boomerang tip of BPI and LBP, consisting of loops 1, 2, and 4 and of helix α2 (as defined in Fig. 1), contains several positively charged residues. These residues are not conserved in PLTP, because the corresponding region contains a hydrophobic cluster of aromatic residues, Tyr-45, Tyr-90, Trp-91, Phe-92, Phe-93, and Tyr-94 (Fig. 2*A*). Fig. 2 (*B* and *C*) shows the electrostatic surface potentials around the BPI crystal structure and the PLTP model. Fig. 2 (*D* and *E*) shows the corresponding surface hydrophobicity around BPI and PLTP. The most striking difference between the BPI structure and the PLTP model lies within the N-terminal boomerang tip of the proteins. In this region, BPI shows a strongly positive electrostatic potential and low surface hydrophobicity (Fig. 2, *B* and *D*), whereas the corresponding region in PLTP has high surface hydrophobicity and a weakly positive electrostatic potential (Fig. 2, *C* and *E*). This is due to the replacement of positively charged residues of BPI by hydrophobic residues in PLTP (Fig. 1). Because the positively charged residues in the N-terminal boomerang tip of LBP are involved in binding of negatively charged LPS, we hypothesized that the corresponding hydrophobic region in PLTP might play a role in substrate binding through hydrophobic interactions. Fig. 3 shows the conformation of the N-terminal tip of the PLTP model after optimization by molecular dynamics simulation. The aromatic residues Tyr-45, Tyr-90,

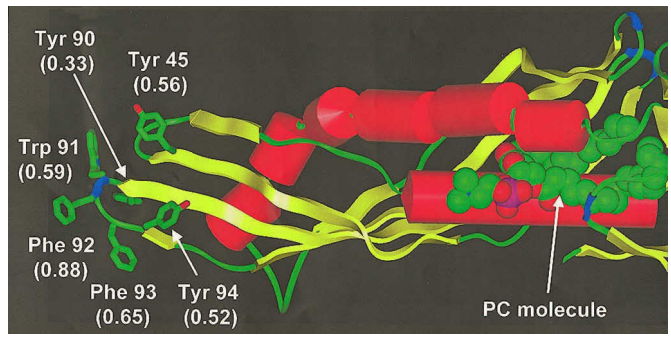

FIG. 3. **Structure of the N-terminal tip of the PLTP molecule.** This figure shows the clustering of aromatic residues Tyr-45, Tyr-90, Trp-91, Phe-92, Phe-93, and Tyr-94 at the N-terminal tip of the boomerang-shaped PLTP and the solvent-exposed orientation of Trp-91, Phe-92, and Phe-93 residues. The indexes of solvent exposure of the residues are indicated in *parentheses*.

Trp-91, Phe-92, Phe-93, and Tyr-94 are solvent-exposed, with solvent accessibility values of 0.56, 0.33, 0.59, 0.88, 0.65, and 0.52, respectively. These residues were separately mutated to an alanine.

Expression of Recombinant Human PLTP by COS-1 Cells—The kinetics of PLTP secretion by COS-1 cells were monitored by assaying PLTP activity in the cell culture media 24, 48, 72, and 96 h after transfection. As shown in Fig. 4, a time-dependent increase in PLTP activity was observed in the culture media of transfected cells, with a maximal increase 72–96 h post-transfection. As PLTP mass was only detected 96 h after transfection by Western blot analysis of cell culture media, and all media were harvested 4 days post-transfection. The specific activity of recombinant wild-type (WT) PLTP expressed as activity/μg of PLTP protein was ~60 nmol/μg/h, compared with about 100 nmol/μg/h for plasma PLTP.

All PLTP mutants were efficiently expressed, at levels above 65% of WT PLTP. The concentration of recombinant PLTP in the cell culture media was around 1 μg/ml (0.9 $\pm$ 0.1, 0.6 $\pm$ 0.2, 0.6 $\pm$ 0.2, 1.0 $\pm$ 0.1, 1.0 $\pm$ 0.2, 0.9 $\pm$ 0.2, and 0.6 $\pm$ 0.1 μg/ml for WT, Y45A, Y90A, W91A, F92A, F93A, and Y94A mutants, respectively).

Phospholipid Transfer Activity of WT and PLTP Mutants—The kinetic parameters for phospholipid transfer from liposomes to various lipoprotein substrates were measured for the engineered PLTP mutants.

We first measured PLTP-mediated transfer of pyrene-labeled phosphatidylcholine from donor liposomes to HDL acceptors. The specific transfer activities of all mutants were calculated based upon the PLTP concentration in the media. Except for the Y45A and Y94A variants, whose specific activity was not statistically different from that of WT PLTP, all single point mutations substantially decreased PLTP-specific activity in the liposome/HDL transfer assay (Fig. 5*A*). The activity of the Y90A variant decreased most, because it amounted only to 30% that of WT PLTP. Mutations of residues Trp-91, Phe-92, and Phe-93 decreased the specific PLTP activity by up to 60%.

To determine whether the reduced activity of the mutants was primarily due to their decreased interaction with liposomes and/or with HDL particles, we modified the liposome/HDL transfer assay into an HDL/HDL transfer assay. Pyrene-labeled HDL were used as phospholipid donors, unlabeled HDL were used as acceptors, and PLTP activity was quantified by measuring the decrease in excimer/monomer fluorescence intensity in HDL. The specific activities of WT and PLTP mutants in this assay system are shown in Fig. 5*B*. They are well correlated with the activities measured with the liposomes/HDL transfer system (r^2 = 0.80). Interestingly, the relative specific activities of the deficient mutants were slightly reduced

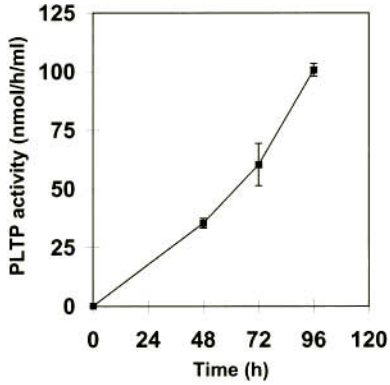

FIG. 4. **Kinetics of PLTP secretion by transiently transfected COS-1 cells.** Aliquots of the cell culture medium of PLTP-transfected COS-1 cells were removed 24, 48, 72, and 96 h post-transfection. The secretion of PLTP by the transfected cells was followed by measuring phospholipid transfer activity from quenched pyrene-labeled liposomes to acceptor HDL in the presence of control medium (mock medium) or PLTP-containing medium. PLTP activities (expressed in nmol/ml/h) are the means ± S.D. of three determinations and were obtained after subtraction of control values.

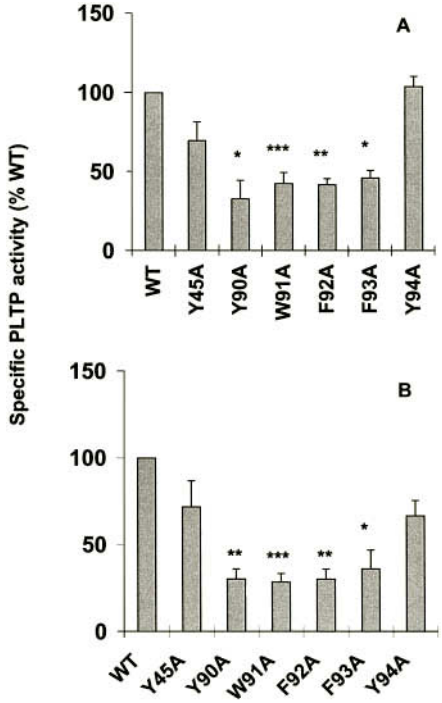

FIG. 5. **Specific phospholipid transfer activity of wild-type and PLTP mutants toward HDL particles.** Phospholipid transfer activity was measured in the cell medium 96 h post-transfection, either from liposomes toward HDL (*A*) or between HDL particles (*B*). Specific phospholipid transfer activities were calculated by taking into account the expression levels of the various transfectants. The results are mean values ± S.E. of three independent experiments and are expressed as percentages of the activity of wild-type PLTP with *, $p < 0.05$; **, $p < 0.01$; and ***, $p < 0.005$ compared with WT PLTP activity (Student's t test).

in the HDL/HDL compared with the liposomes/HDL assay, suggesting that the functional defect of the mutants primarily lies in a decreased interaction with HDL substrates.

To investigate whether these clustered aromatic residues might also be involved in the interaction of PLTP with VLDL and LDL, the specific phospholipid transfer activity of the WT PLTP and of PLTP mutants was determined by using liposomes as donors and VLDL or LDL particles as acceptors. As shown in Table I, only the Y90A mutant showed a significantly reduced ability to transfer phospholipids from liposomes to VLDL or LDL; all other PLTP mutants displayed a normal or even slightly increased specific phospholipid transfer activity toward VLDL and LDL, suggesting that mutation of Trp-91, Phe-92, and Phe-93 specifically impairs the interaction of PLTP with HDL particles.

Effect of Salt Concentrations on PLTP Activity—To investigate the contribution of electrostatic and hydrophobic forces to the activity of WT PLTP and of PLTP mutants, the effect of ionic strength on phospholipid transfer from donor liposomes to either VLDL, LDL, or HDL was measured. PLTP activity was hardly detectable when the assay was performed in 1 mM EDTA, however, it was markedly enhanced in the presence of 10 mM Tris/HCl buffer, as previously observed for CETP (35). In assays carried out in the presence of 10 mM Tris-HCl buffer (Fig. 6*A*), phospholipid transfer from liposomes to HDL was markedly increased when the NaCl concentration was decreased from 150 to 50 mM. Phospholipid transfer from liposomes to VLDL and LDL particles was also enhanced upon decreasing NaCl concentrations, although to a lesser extent than with HDL acceptors. The effect of decreasing NaCl concentrations on phospholipid transfer from liposomes to HDL was more pronounced for the W91A, F92A, and F93A PLTP mutants, compared with WT PLTP (Fig. 6*B*). The increase in phospholipid transfer from liposomes to VLDL and LDL was similar for all PLTP variants (results not shown). The phospholipid transfer activity from liposomes to VLDL, LDL, or HDL particles measured for the Y94A mutant was similar to that of WT PLTP (Fig. 6*B*). In experiments performed with egg PC liposomes instead of PC/PS liposomes, a similar trend was observed (data not shown).

HDL Size Conversion by WT and PLTP Mutants—Changes in the size distribution of HDL particles by recombinant wild-type and PLTP mutants were investigated. Isolated plasma HDL were incubated with either mock- or PLTP-transfected culture media, containing identical amounts of WT PLTP or PLTP mutants, for 30 h at 37 °C. The mixtures were then subjected to density gradient ultracentrifugation, to determine the density of the incubated HDL, together with the amount of released apoAI. As shown in Fig. 7, HDL particles incubated in the presence of control medium were isolated in the 1.07–1.15 g/ml density range; after incubation with PLTP, the HDL peak was shifted to lower densities (1.05–1.10 g/ml), illustrating formation of apoAI-depleted, larger-sized HDL particles. Concomitant release of lipid-poor apoAI was observed in the $d >$ 1.20 g/ml fraction. The apoAI release in the bottom fraction of the gradient was used as a quantitative measure of PLTP conversion activity. Table II shows the effect of PLTP concentration on apoAI release. The experimental data were fitted to a linear equation ($y = 0.41x + 10$, $r^2 = 0.86$), which was used to calculate the specific conversion activities of the PLTP mutants. As shown in Table III, mutants Y90A, W91A, F92A, and F93A only displayed 46, 37, 26, and 61% of WT specific conversion activity, whereas Y45A and Y94A mutations did not markedly impair the HDL size conversion activity of PLTP. The HDL size conversion was also verified by native polyacrylamide gradient gel electrophoresis as described by other groups (36, 37). Changes in HDL size upon incubation with WT PLTP are represented in Fig. 8. The sizes of the HDL subfractions measured after incubation with mock medium were: 58% particles with a diameter of 9.6 nm; 42% of 8.5 nm, and no smaller sized particles (7.8 nm). After incubation with WT PLTP, 63% of the particles had an average size of 9.6 nm; 25% of 8.5 nm, and 12% had a size of 7.8 nm. This size distribution is in accordance with the changes in density of the HDL particles as described in Fig. 7.

TABLE I
Relative specific activity (% of wild-type, mean ± S.E.) in cell media from wild-type and mutant PLTP transfectants

Transfectant	Specific phospholipid transfer activity			
	Liposomes→HDL	HDL→HDL	Liposomes→VLDL	Liposomes→LDL
		%		
Wild-type	100	100	100	100
Y45A	69.7 ± 8.9	71.9 ± 15.1	151.8 ± 11.7[a]	81.4 ± 6.5
Y90A	32.9 ± 11.6[a]	30.4 ± 5.7[b]	<10	<10
W91A	42.6 ± 3.9[c]	28.6 ± 4.9[c]	107.6 ± 22.5	119.2 ± 11.0
F92A	41.8 ± 4.8[b]	30.2 ± 5.7[b]	115.1 ± 22.8	110.5 ± 8.5
F93A	46.1 ± 6.4[a]	36.1 ± 10.8[a]	149.5 ± 11.7	148 ± 18.0
Y94A	104.1 ± 6.9	66.6 ± 8.8	79.44 ± 11.9	128.2 ± 22.4

[a] $p < 0.05$; [b] $p < 0.01$; and [c] $p < 0.005$ *versus* wild-type activity.

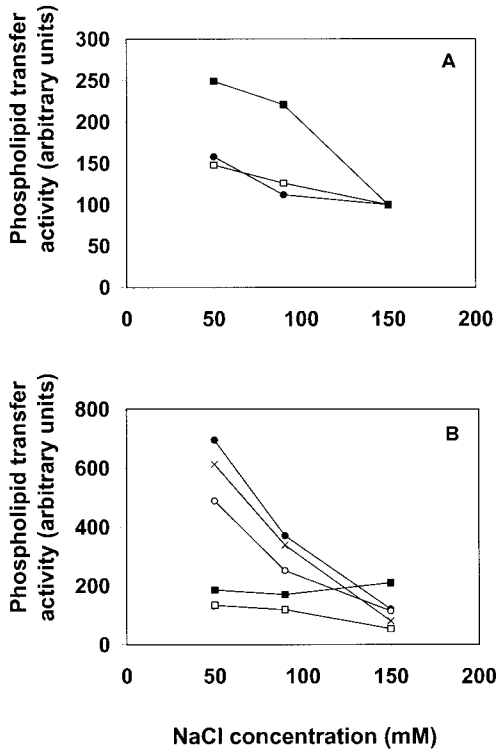

FIG. 6. **Effect of sodium chloride concentration on PLTP-mediated phospholipid transfer.** *A*, phospholipid transfer was measured in assay mixtures containing donor liposomes (12 nmol of phospholipids), acceptor lipoproteins (80 nmol of phospholipids), and control or PLTP-containing cell culture medium. NaCl concentrations were adjusted with 10 mM Tris/NaCl solutions. Each *point* is the mean of two determinations. PLTP activity in the presence of acceptor VLDL (●), LDL (□), and HDL (■) particles. *B*, phospholipid transfer was measured in assay mixtures containing donor liposomes (12 nmol of phospholipids), acceptor HDL (80 nmol of phospholipids), and control or PLTP-containing cell culture medium. The experiment was conducted either with WT PLTP or with PLTP mutants. Each *point* is the mean of two determinations: WT PLTP (□); W91A mutant (X); F92A mutant (○); F93A mutant (●); Y94A mutant (■).

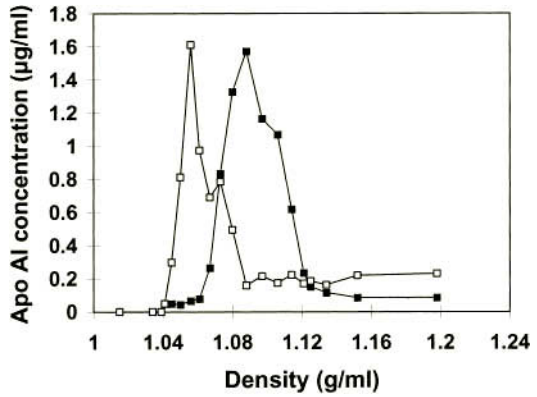

FIG. 7. **Density gradient ultracentrifugation profile of HDL incubated with mock medium (■) or with PLTP-containing medium (□).** The position of the HDL peaks was identified by measuring the apoAI concentration (μg/ml) in each fraction.

TABLE II
Size conversion activity of wild-type recombinant PLTP as assessed by apoAI release

Isolated HDL were incubated with control or PLTP-containing cell culture media for 30 h at 37 °C. The percentage of apoAI released in the bottom fraction of ultracentrifuged mixtures was used to quantitate the HDL size conversion activity of recombinant PLTP.

Standard curve: PLTP activity	ApoAI released (30 h)
nmol/ml/h	%
0	11.3 ± 0.7
10	13.6 ± 1.9
20	15.4 ± 3.1
30	24.3 ± 2.1

TABLE III
Size conversion activity of wild-type and mutant forms of PLTP as assessed by apoAI release

Isolated HDL were incubated with control or PLTP-containing cell culture media for 30 h at 37 °C. The volumes of cell culture media were adjusted so as to contain the same amounts of WT PLTP or PLTP mutants. The percentage of apoAI released in the bottom fraction of ultracentrifuged mixtures was used to quantitate the HDL size conversion activity of PLTP.

PLTP transfectant	Specific conversion activity
	% of wild-type
Wild-type	100
Y45A	82 ± 6
Y90A	46 ± 11
W91A	37 ± 9
F92A	26 ± 1
F93A	61 ± 10
Y94A	93 ± 17

DISCUSSION

The molecular and macromolecular specificity of PLTP has recently been thoroughly investigated (18–21). Phospholipid transfer activity depends upon the size, composition, fluidity (19, 21), and electrostatic charge (38) of the lipoprotein substrates. HDL particles are the preferential substrates for PLTP (21). Because the PLTP structure has not yet been determined, the molecular basis for PLTP specificity is not known. The results reported here are a new experimental link between PLTP structure and macromolecular specificity.

We first performed a multiple sequence alignment to assess the degree of residue conservation among the members of the LT/LBP family. Residue conservation within members of this family is low, around 20%. Residues in the secondary structure elements of BPI are, however, well conserved, enabling molecular modeling of PLTP, using BPI as a template. As described by Huuskonen *et al.* for PLTP (22) and by Bruce *et al.* for CETP

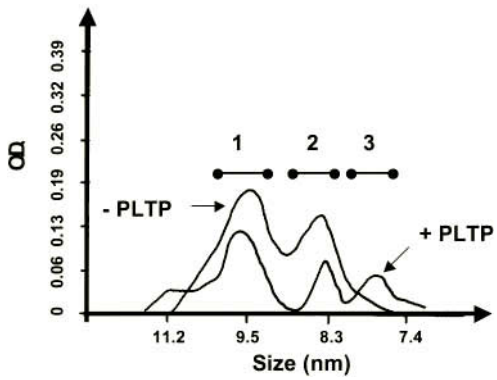

FIG. 8. **Effect of incubation with PLTP on the HDL size distribution as determined by native density gradient (4–20%) gel electrophoresis.** HDL were incubated with mock medium or with medium containing WT PLTP as described under "Materials and Methods." *1*, a size of 9.6 nm; *2*, 8.5 nm; and *3*, 7.8 nm.

(15), the major structural elements and the functional lipid-binding pockets inside the anti-parallel barrel structures are well conserved. Because our sequence alignments are practically identical to those of Huuskonen *et al.* (22), both PLTP models share high similarity.

In this study, a cluster of positively charged residues was identified on the N-terminal boomerang tip of BPI. In LBP, these residues were shown to be critical for its interaction with bacterial lipopolysaccharides (16). The multiple sequence alignment indicated that these residues are not conserved in PLTP. Residues Lys-95, Arg-96, and Lys-99 in BPI are replaced by Tyr-90, Trp-91, and Tyr-94 in PLTP. Analysis of the PLTP model showed that these residues, together with the adjacent residues Phe-92 and Phe-93, as well as Tyr-45, form a highly hydrophobic patch exposed at the N-terminal tip of the PLTP molecule. We therefore speculated that at least some of these hydrophobic residues might play a specific role in the activity of PLTP, and we tested this hypothesis by site-directed mutagenesis.

Mutation of residues Trp-91, Phe-92, and Phe-93, but not Tyr-45 and Tyr-94, decreased the specific phospholipid transfer activity of PLTP from donor liposomes to HDL by up to 60%. The decreased transfer activity of the PLTP mutants on HDL was confirmed in a new assay system, where HDL served both as phospholipid donors and acceptors for PLTP-mediated transfer. In contrast, when VLDL or LDL particles were used as acceptors in the transfer assay, the specific PLTP activity of the five mutants was not different from that of WT PLTP. This observation indicates that the nature of acceptor lipoproteins is critical for phospholipid transfer by the W91A, F92A, and F93A PLTP mutants. Mutation Y90A affected PLTP-mediated transfer of phospholipids to VLDL, LDL, and HDL lipoproteins. Because Tyr-90 is less solvent-exposed than the other mutated residues in the PLTP model (Fig. 3), this residue is more likely involved in stabilizing hydrophobic intramolecular interactions, whose impairment might account for the loss of PLTP activity of the Y90A mutant, in all assays.

Because residues Trp-91, Phe-92, and Phe-93 seem critical for phospholipid transfer to HDL particles, they might also influence the HDL size conversion activity of PLTP. We observed a close parallel between HDL conversion and phospholipid transfer activities of the mutants, suggesting that both processes are linked. This observation strongly supports the sequential mechanism recently proposed by Lusa *et al.* (39), in which PLTP-mediated phospholipid transfer is a prerequisite for HDL fusion. According to this hypothesis, redistribution of phospholipid molecules among HDL particles would induce dissociation of apoAI molecules from HDL surface, followed by destabilization of surface-depleted HDL particles. This would enhance HDL fusion into larger particles. The cluster of hydrophobic residues mutated in this study might play a role in the displacement of apoAI from the HDL surface, possibly by penetrating deeply into the outer phospholipid layer and increasing surface pressure on HDL.

The detailed mechanism of PLTP-mediated phospholipid transfer is still unknown. Studies of the mechanism of action of the related CETP protein (1, 6, 35) have stressed the importance of two events for lipid transfer activity: (i) interaction of the transfer protein with donor and acceptor substrate particles and (ii) binding and accommodation of substrate lipid molecules in CETP. The decreased activity of the PLTP mutants generated in this study might be due either to decreased interactions with donor and/or acceptor lipoprotein particles or to a decreased ability to accommodate phospholipids in the lipid-binding pockets (22). A decreased interaction of the PLTP mutants with phospholipids would have affected phospholipid transfer activity from liposomes to all lipoprotein acceptors. In contrast, the transfer activity of the mutants was close to that of WT PLTP for liposomes/VLDL and liposomes/LDL assays. This suggests that all mutants (except Y90A) interact normally with donor liposomes, and efficiently transfer phospholipids from these particles. Mutation of residues Trp-91, Phe-92, or Phe-93, which appear as the most protruding and solvent-exposed residues in the optimized conformation of the PLTP N-terminal tip (Fig. 3), prevented PLTP-mediated transfer of phospholipids toward HDL. This observation suggests that these residues might be specifically involved in hydrophobic interactions between PLTP and HDL particles.

We previously showed that electrostatic interactions can also contribute to PLTP-HDL association (38). The relative importance of electrostatic and hydrophobic interactions for HDL-PLTP association was investigated by performing phospholipid transfer measurements at varying salt concentrations. We first observed that addition of Tris-HCl ions to the assay mixtures increased PLTP transfer activity, probably through increased hydrophobic interactions (35). Moreover, increasing electrostatic interactions by decreasing NaCl concentrations below physiological range also enhanced phospholipid transfer, especially from liposomes (both PC only and PC/PS liposomes) to HDL. This effect was most pronounced for the W91A, F92A, and F93A mutants, where the contribution of hydrophobic interactions with HDL had been reduced by mutations of the aromatic residues to alanine. These observations thus support the assumption that Trp-91, Phe-92, and Phe-93 contribute to hydrophobic interactions between PLTP and HDL particles, that constitute a rate-limiting factor for PLTP activity at physiological ionic strength. At lower ionic strength, electrostatic interactions might compensate for the impaired hydrophobic interactions in the engineered mutants.

Residues Trp-91, Phe-92, and Phe-93 might play a role in the interaction of PLTP with either apolipoprotein AI or other HDL protein components (40). However, because aromatic residues are known to be frequently involved in protein-lipid interactions (41), the mutated aromatic residues in PLTP probably contribute to hydrophobic interactions with HDL lipids. Lookene *et al.* (42) recently demonstrated the contribution of aromatic residues for the interaction of lipoprotein lipase with an interfacial substrate. The interfacial binding domain of snake venom phospholipase A2 also contains several solvent-exposed hydrophobic residues. Depending on their location and side-chain orientation, aromatic Trp, Tyr, and Phe residues can significantly contribute to interfacial binding (43). Studies of the PLA_2 family showed that, although electrostatic interactions between basic residues and anionic phospholipids account

for high affinity binding of some of these enzymes, hydrophobic residues in the interfacial binding domain enhance interaction with neutral lipid substrates (44, 45). In analogy with the phospholipase A2 family, the presence of a solvent-exposed hydrophobic cluster is a specific feature of PLTP within the LT/LBP family, whereas the corresponding positively charged domains constitute the lipopolysaccharide-binding domain in LBP and BPI (16).

Activity measurements performed with the PLTP mutants suggest that the nature of lipoprotein substrates, and especially their physicochemical properties, determines relative transfer activities. Differences in the molecular packing of surface lipids were shown to determine the lipoprotein specificity of apolipoproteins (46, 47) and of lipolytic enzymes (48, 49). Ibdah *et al.* (50) demonstrated a denser phospholipid packing on the surface of LDL relative to HDL particles. Phospholipid packing might therefore influence the depth of insertion of the bulky hydrophobic residues of PLTP between the polar headgroups of the phospholipid monolayer. Binding of lipolytic enzymes to their substrates can potentially cause protein denaturation. Therefore, the structure of these proteins is stabilized against denaturation by disulfide bridges in phospholipases A2 and by buried salt bridges in fungal lipases. In the PLTP model, a buried salt bridge was detected between the conserved residues arginine 86 and aspartic acid 94, which are on the adjacent beta-strands β4 and β5. This salt bridge, which is not conserved in other members of the LT/LBP family, might help to stabilize the PLTP structure. This hypothesis could be tested experimentally, by site-directed mutagenesis and expression of the mutants.

In conclusion, the results of the present study show that phospholipid transfer and size conversion activities of PLTP on HDL are influenced by mutation of three aromatic residues (Trp-91, Phe-92, and Phe-93), predicted to be solvent-exposed in an hydrophobic patch located at the N-terminal tip of the molecule. These protruding residues might be critically involved in the interaction of PLTP with HDL. Huuskonen *et al.* (22) recently demonstrated that the interaction of PLTP with HDL involves Leu-286, which is located in the central part of the concave surface of PLTP. In contrast, mutations in the N-terminal pocket decreased phospholipid transfer activity but not HDL binding (22). Deletion of the 30 C-terminal residues 464–493 did not affect secretion of PLTP but decreased the activity (51). The contribution of Phe-464, located at the entrance of the N-terminal lipid-binding pocket, for the proper conformation of the C-terminal tail of PLTP was clearly demonstrated in the same study (22). Taken together, these data and our present observations support the existence of at least two distinct HDL-binding sites on PLTP, suggesting that PLTP-mediated lipid transfer occurs through formation of collisional ternary complexes rather than through a "shuttle" mechanism. Moreover, PLTP-mediated size conversion of HDL particles, which results from particle fusion, might be enhanced by the bridging ability of PLTP through inter-particle contacts in the aqueous phase. Experimental determination of the kinetics of PLTP activity could contribute toward the unraveling of the structure/function relationship of PLTP.

Acknowledgments—We are grateful to Drs. J. J. Albers and A.-Y. Tu (Seattle, WA) for providing the PLTP14 template vector, and to Dr. L. Lagrost (Dijon, France) who generously provided the anti-PLTP antibodies. Hans Caster is acknowledged for his expert technical assistance.

REFERENCES

1. Bruce, C., Chouinard, R. A., and Tall, A. R. (1998) *Annu. Rev. Nutr.* **18,** 297–330
2. Lagrost, L., Desrumaux, C., Masson, D., Deckert, V., and Gambert, P. (1998) *Curr. Opin. Lipidol.* **9,** 203–209
3. Huuskonen, J., and Ehnholm, C. (2000) *Curr. Opin. Lipidol.* **11,** 285–289
4. Lagrost, L. (1997) *Trend. Cardiovasc. Med.* **7,** 218–224
5. Day, J. R., Albers, J. J., Lofton-Day, C. E., Gilbert, T. L., Ching, A. F. T., Grant, F. J., O'Hara, P. J., Marcovina, S. M., and Adolphson, J. L. (1994) *J. Biol. Chem.* **269,** 9388–9391
6. Lagrost, L. (1994) *Biochim. Biophys. Acta* **1215,** 209–236
7. Schumann, R. R., Leong, S. R., Flaggs, G. W., Gray, P. W., Wright, S. D., Mathison, J. C., Tobias, P. S., and Ulevitch, R. J. (1990) *Science* **249,** 1429–1431
8. Weiss, J., Muello, K., Victor, M., and Elsbach, P. (1984) *J. Immunol.* **132,** 3109–3115
9. Beamer, L. J., Carroll, S. F., and Eisenberg, D. (1998) *Protein Sci.* **7,** 906–914
10. Beamer, L. J., Carroll, S. F., and Eisenberg, D. (1997) *Science* **276,** 1861–1864
11. Schumann, R. R., and Latz, E. (2000) *Chem. Immunol.* **74,** 42–60
12. Ooi, C. E., Weiss, J., and Elsbach, P. (1991) *Agents Actions* **34,** 274–277
13. Abrahamson, S. L., Wu, H. M., Williams, R. E., Der, K., Ottah, N., Little, R., Gazzano-Santoro, H., Theofan, G., Bauer, R., Leigh, S., Orme, A., Horwitz, A. H., Carroll, S. F., and Dedrick, R. L (1997) *J. Biol. Chem.* **272,** 2149–2155
14. Wiese, A., Brandenburg, K., Carroll, S. F., Rietschel, E. T., and Seydel, U. (1997) *Biochemistry* **36,** 10311–10319
15. Bruce, C., Beamer, L. J., and Tall, A. R. (1998) *Curr. Opin. Struct. Biol.* **8,** 426–434
16. Lamping, N., Hoess, A., Yu, B., Park, T. C., Kirschning, C.-J., Pfeil, D., Reuter, D., Wright, S. D., Herrmann, F., and Schumann, R. R. (1996) *J. Immunol.* **157,** 4648–4656
17. Beamer, L. J., Carroll, S. F., and Eisenberg, D. (1999) *Biochem. Pharmacol.* **57,** 225–229
18. Massey, J. B., Hickson-Bick, D., Via, D. P., Gotto, A. M., Jr, and Pownall, H. J. (1985) *Biochim. Biophys. Acta* **835,** 124–131
19. Sweeny, S. A., and Jonas, A. (1985) *Biochim. Biophys. Acta* **835,** 279–290
20. Huuskonen, J., Olkkonen, V. M., Jauhiainen, M., Metso, J., Somerharju, P, and Ehnholm, C. (1996) *Biochim. Biophys. Acta* **1303,** 207–214
21. Rao, R., Albers, J. J., Wolfbauer, G., and Pownall, H. J. (1997) *Biochemistry* **36,** 3645–3653
22. Huuskonen, J., Wohlfahrt, G., Jauhiainen, M., Ehnholm, C., Teleman, O., and Olkonnen, V. M. (1999) *J. Lipid Res.* **40,** 1123–1130
23. Thompson, J. D., Higgins, D. G., and Gibson, T. J. (1994) *Nucleic Acids Res.* **22,** 4673–4680
24. Karplus, K., Barrett, C., Cline, M., Diekhans, M., Grate, L., and Hughey, R. (1999) *Proteins* **37,** Suppl. 3, 121–125
25. Karplus, K., Barrett, C., and Hughey, R. (1998) *Bioinformatics* **14,** 846–856
26. Barton, G. J. (1993) *Protein Eng.* **6,** 37–40
27. Livingstone, C. D., and Barton, G. J. (1993) *Comput. Appl. Biosci.* **9,** 745–775
28. Rodriguez, R., Chinea, G., Lopez, N., Pons, T., and Vriend, G. (1998) *Comput. Appl. Biosci.* **14,** 523–528
29. Laskowski, R. A., MacArthur, M. W., Moss, D. S., and Thornton, J. M. (1993) *J. Appl. Crystallogr.* **26,** 283–291
30. Bower, M. J., Cohen, F. E., and Dunbrack, R. L., Jr. (1997) *J. Mol. Biol.* **267,** 1268–1282
31. Desrumaux, C., Athias, A., Bessède, G., Vergès, B., Farnier, M., Perségol, L., Gambert, P., and Lagrost, L. (1999) *Arterioscler. Thromb. Vasc. Biol.* **19,** 266–275
32. Havel, R. J., Eder, H. A., and Bragdon, J. H. (1955) *J. Clin. Invest.* **34,** 1345–1353
33. Rosseneu, M., and Bury, J. (1988) *Prog. Clin. Biol. Res.* **255,** 143–154
34. Blanche, P. J., Gong, E. L., Forte, T. M., and Nichols, A. V. (1981) *Biochim. Biophys. Acta* **665,** 408–419
35. Nishida, H. I., Arai, H., and Nishida, T. (1993) *J. Biol. Chem.* **268,** 16352–16360
36. Tu, A. Y., Nishida, H. I., and Nishida, T. (1993) *J. Biol. Chem.* **268,** 23098–23108
37. Jauhiainen, M., Metso, J., Pahlman, R., Blomqvist, S., van Tol, A., and Ehnholm, C. (1993) *J. Biol. Chem.* **268,** 4032–4036
38. Desrumaux, C., Athias, A., Masson, D., Gambert, P., Lallemant, C., and Lagrost, L. (1998) *J. Lipid Res.* **39,** 131–142
39. Lusa, S., Jauhiainen, M., Metso, J., Somerharju, P., and Ehnholm, C. (1996) *Biochem. J.* **313,** 275–282
40. Pussinen, P. J., Jauhiainen, M., Metso, J., Pyle, L. E., Marcel, Y. L., Fidge, N. H., and Ehnholm, C. (1998) *J. Lipid Res.* **39,** 152–161
41. Wimley, W. C., and White, S. H. (1996) *Nat. Struct. Biol.* **3,** 842–848
42. Lookene, A., Groot, N. B., Kastelein, J. J. P., Olivecrona, G., and Bruin, T. (1997) *J. Biol. Chem.* **272,** 766–772
43. Sumandea, M., Das, S., Sumandea, C., and Cho, W. (1999) *Biochemistry* **38,** 16290–16297
44. Janssen, M. J. W., Burghout, P. J., Verheij, H. M., Slotboom, A. J., and Egmond, M. R. (1999) *Eur. J. Biochem.* **263,** 782–788
45. Gelb, M. H., Cho, W., and Wilton, D. C. (1999) *Curr. Opin. Struct. Biol.* **9,** 428–432
46. Ibdah, J. A., and Phillips, M. C. (1988) *Biochemistry* **27,** 7155–7162
47. Wetterau, J. R., and Jonas, A. (1982) *J. Biol. Chem.* **257,** 10961–10966
48. Jackson, R. L., McLean, L. R., and Demel, R. A. (1987) *Am. Heart J.* **113,** 551–554
49. Tansey, J. T., Thuren, T. Y., Jerome, W. G., Hantgan, R. R., Grant, K., and Waite, M. (1997) *Biochemistry* **36,** 12227–12234
50. Ibdah, J. A., Lund-Katz, S., and Phillips, M. C. (1989) *Biochemistry* **28,** 1126–1133
51. Huuskonen, J., Jauhiainen, M., Ehnholm, C., and Olkkonen, V. M. (1998) *J. Lipid Res.* **39,** 2021–2030
52. Gilson, M. K., and Honig, B. (1988) *Proteins* **4,** 7–18